CSF1R-Related Leukoencephalopathy Caused by CSF1R p.Arg777Trp and CSF1R p.Arg782Cys Mutations: A Report of Four Cases in Sweden

Igal Rosenstein
University of Gothenburg Institute of Neuroscience and Physiology: Goteborgs universitet Institutionen for neurovetenskap och fysiologi
Oluf Andersen
Sahlgrenska University Hospita, Department of Neurology
Victor Daniel
Lanssjukhuset i Halmstad: Hallands sjukhus Halmstad
Elisabet Englund
Lunds Universitet
Tobias Granberg
Karolinska Universitetssjukhuset Neuroradiologiska kliniken
Carola Hedberg-Oldfors
Institute of Biomedicine, University of Gothenburg:
Katarina Jood
Sahlgrenska University Hospital: Sahlgrenska universitetssjukhuset
Yusran Ady Fitrah
Niigata University: Niigata Daigaku
Takeshi Ikeuchi
Niigata University: Niigata Daigaku
Virginija Danylaité Karrenbauer (virginija.karrenbauer@ki.se)
Karolinska Institutet Institutionen for klinisk neurovetenskap https://orcid.org/0000-0002-7166-8951

Research article

Keywords: Adult-onset leukoencephalopathy with spheroids and pigmented glia, biomarkers, neurodegeneration, colony stimulating factor 1 receptor, CSF1R gene, primary microgliopathy

Posted Date: July 20th, 2021

DOI: https://doi.org/10.21203/rs.3.rs-718394/v1

Abstract

Background: Colony stimulating factor 1 receptor (*CSF1R)*-related leukoencephalopathy is a rare and devastating genetic disease caused by heterozygous mutations in the *CSF1R* gene. It is characterized by adult onset, rapidly progressive neurodegeneration and variable behavioral, cognitive, and motor disturbances and seizures. With only one affected family currently reported, the disease's prevalence in Sweden is unknown.

Objective: To describe four cases of *CSF1R*-related leukoencephalopathy from three families with two different pathogenic mutations in the tyrosine kinase domain of *CSF1R* and to develop an integrated presentation of inter-individual diversity of clinical presentations.

Methods: This is an observational study of a case series. Patients diagnosed with *CSF1R*-encephalopathy were evaluated with standardized functional estimation scores and analysis of cerebrospinal fluid biomarkers. Brain computed tomography (CT) and magnetic resonance imaging (MRI) were systematically evaluated. We performed a functional phosphorylation assay to confirm the pathogenicity of the mutations. We performed neuropathologic examination on one deceased relative for diagnostic verification.

Results: Two mutationsin *CSF1R* gene were identified, a missense variant c.2344C>T, p.Arg782Cys and a missense variant c.2329C>T, p.Arg777Trp. A phosphorylation assay *in vitro* showed markedly reduced autophosphorylation in cells expressing the CSF1R mutations p.Arg777Trp and p.Arg782Cys, confirming the pathogenicity of these mutations. A radiological investigation revealed typical white matter lesions in all cases. There was marked individual variation in the loss of frontal, motor neuronal and extrapyramidal functions, with a reciprocal relation to neurofilament light levels in the cerebrospinal fluid.

Conclusions: Including the present cases, currently three *CSF1R* mutations are known in Sweden. We present a visualization tool to capture the degree of disability and clinical diversity, with a potential use for longitudinal follow-up for this and other leukoencephalopathies.

Trial Registration: N/A (non-interventional study)

Background

The *CSF1R* gene on chromosome 5q32 encodes a receptor for colony stimulating factor 1, which regulates the function and maturation of the monocyte/macrophage lineage, including microglia (1). The receptor is also expressed in osteoclasts and plays an important role in bone mineralization (2). Heterozygous mutations in this gene have been identified in patients with autosomal dominant adult-onset leukoencephalopathy with axonal spheroids and pigmented glia (ALSP), which includes hereditary diffuse leukoencephalopathy with spheroids (HDLS) and pigmentary orthochromatic leukodystrophy [POLD, (3)]. Recent genetic data and common neuropathology confirm that HDLS and POLD constitute a single nosological unit (4), now termed *CSF1R*-related leukoencephalopathy. It is characterized by rapidly progressive neurodegeneration and variable behavioral, cognitive and motor disturbances as well as seizures. In the last stage of the disease, affected individuals become bedridden with spasticity and progress

to a vegetative state (5). Mean age at onset is in the fourth decade, and the disease course ranges from two to thirty years (5). Brain magnetic resonance imaging (MRI) typically shows progressive bifrontal and biparietal cerebral white matter abnormalities in the subcortical and periventricular regions (6). To date, 71 different *CSF1R* mutations (56 missense mutations, 8 splice-site mutations, 3 frameshift mutations, 2 nonsense mutations, and 2 small deletions) have been described (7), but the true prevalence and incidence of the disease is still unknown.

In this study, we describe four cases from three families with two different pathogenic mutations in the tyrosine kinase domain of *CSF1R.* We capture the range of clinical presentations, using several standardized scoring scales to facilitate a description of individual disease trajectories.

Material And Methods

Patients

Patients were initially assessed at their local hospitals according to each clinic's routine. All patients were diagnosed either with definitive ALSP (Patients 1, 3 and 4) or probable ALSP (Patient 2) using ALSP diagnostic criteria (8). Comprehensive assessment was performed by the study team using several standardized clinical rating scales to capture the diverging clinical phenotypes: Unified Parkinson's Disease Rating Scale (UPDRS) parts I–VI (9), Amyotrophic Lateral Sclerosis Functional Rating Scale [ALSFRS-R, (10)], Hospital Anxiety and Depression Scale [HADS, (11)], and Expanded Disability Status Scale [EDSS, (12)]. Cognitive status was evaluated with Mini-Mental State Examination [MMSE, (13)], Montreal Cognitive Assessment [MOCA, (14)], and the Symbol Digit Modalities Test [SDMT, (15)]. To estimate quality of life, multiple sclerosis impact scale [MSIS-29, (16)] and EuroQol-dimension [EQ5D/VAS, (17)] scales were used. Computed tomography (CT) and MRI were performed according to clinical routine with different standard scanners and protocols. We systematically re-evaluated all available imaging. Patient 2 succumbed in 1991.

Genetic analysis

Sequence analysis was performed by Blueprint© Genetics using the Leukodystrophy and Leukoencephalopathy panel (Version 3, Mar 01, 2018).

Neuropathological analysis

A neuropathologic examination was performed at autopsy in 1991, and sectioning and staining were renewed in 2020 for this study. Photomicrographs were produced, and the sections were stained by hematoxylin-eosin, Luxol Fast Blue - Cresyl violet and Gallyas silver.

Phosphorylation assay

To assess the pathogenicity of CSF1R p.Arg777Trp and p.Arg782Cys mutants, we performed a functional assay of these mutants, as previously described (18). HEK293T cells were transfected with cDNA encoding p.Arg777Trp and p.Arg782Cys. After 20 min of ligand (CSF1) stimulation, autophosphorylation of CSF1R at residues of Tyr546, Tyr708 and Tyr723 were examined using antibodies against specific phosphorylated CSF1Rs. Statistical analysis was performed with one-way ANOVA using a Tukey multiple comparison test.

Graphical visualization

Graphical visualization of functional estimate scores (ALSP-FES) vs. relative concentration of neurofilament light (NFL) in cerebrospinal fluid (CSF) was performed using Microsoft Excel. Details of calculations and formulas are included in Supplementary Material 2–4.

Ethics

The Swedish Research Ethics Committee (Ref. 2019–05742, March 19, 2020) approved the study. Patients 1, 3 and 4 signed written informed consent. Patient 2 was deceased before the study initiation. Permission was granted by patient 2's family to publish both clinical history and histopathological findings. All procedures were performed in accordance with the principles of the Declaration of Helsinki.

Results

Table 1 summarizes demographic and clinical characteristics of Patients 1–4.

Table 1. Demographics and clinical characteristics of patients included in this study

Patient Variable	Patient 1	Patient 2	Patient 3	Patient 4
Age at symptom onset	41	42	42	48
Presenting symptoms	Frontal	Frontal	Hemiparesis	Bulbar
Sex	Male	Female	Female	Male
Ethno-regional descent	Nordic	Nordic	Nordic	Nordic
Mutation position	5:149435880	N/A	5:149435895	5:149435895
Mutation	Heterozygous missense variant c.2344C>T	N/A	Heterozygous missense variant c.2329C>T	Heterozygous missense variant c.2329C>T
Amino acid exchange	p.Arg782Cys	N/A	p.Arg777Trp	p.Arg777Trp
Diagnosis according to ALSP diagnostic criteria (5, 8)	Definitive ALSP 2a, 2b, 3, 4a	Possible ALSP 2a, 3, 4a	Definitive ALSP 2a, 2b, 3, 4a	Definitive ALSP 2a, 2b, 2c, 3, 4a

Abbreviations: N/A = Not Available; Arg = Arginine; Cys = Cysteine; Trp = Tryptophan; ALSP = Adult Leukoencephalopathy with Spheroids and Pigmented glia.

Individual description of cases

Patient 1. A 41-year-old previously healthy man of Nordic ethnicity was admitted to a local hospital for sepsis and erysipelas of the arm. Hospital staff noted abnormal social behavior, reduced speech fluency and

verbal response latency. Brain CT revealed moderate periventricular and frontal white matter lesions and small frontal calcifications bilaterally (Figure 1A). Family members confirmed progressive cognitive and neuropsychiatric decline over the past year, including personality changes with agitation, apathy, anxiety and emotional lability. There was no history of substance abuse. Neurological assessment revealed moderate dysarthria and reduced speech fluency but no other neurological deficits. At clinical 10-month follow-up, speech modalities had declined. The patient had increased tonus in all extremities and spastic gait. At our 2-year follow-up, the patient lived in a nursing home. Neurological examination revealed significant deterioration with dementia, mutism, choreoathetoid movements, and a complex motor pyramidal–extrapyramidal syndrome. Neuropsychiatric assessment showed reduced attention, information processing, verbal and visuospatial abilities, verbal and visual memory, and executive skills. Relatives reported reduced school performance. The patient was suspected to have had a neuropsychiatric disturbance long before a full-blown neurodegenerative process developed. (A complete summary of the neuropsychiatric assessment is given in Supplementary Material 1). A brain MRI demonstrated confluent, symmetric, bifrontoparietal white matter changes (WMC) with a clear U-fiber sparing (Figure 1A). The lesions showed pronounced low T1 signal, indicative of marked demyelination. There was also central atrophy with enlarged ventricles and thinning of corpus callosum. A follow-up brain MRI 10 months later revealed progression of WMC and a global cortical atrophy (GCA) scale (19) rating of 2. There was no history of neurological hereditary diseases. Both parents were alive and healthy at the time of presentation. The Blueprint Genetics© *CSF1R* single gene test (Version 1, Mar 01, 2018) Plus Analysis identified a missense variant c.2344C>T, p.Arg782Cys.

Patient 2. A 42-year-old woman of Nordic ethnicity was admitted to a psychiatric clinic with a few months' history of depersonalization and cognitive dysfunction. Both parents were alive without any known neurological diseases. She had psoriasis but no other medical history. Neurological examination was normal except for positive glabellar reflex and muscular jerkiness. She was initially diagnosed with depression. Testing revealed lack of emotional contact, confabulation tendency, symptom denial, reduced concentration and endurance, and dysphasia. Proposed diagnosis was frontal lobe dementia. Brain CT showed atrophy, most pronounced in the frontal lobes. MRI showed atrophy and widespread, mostly frontal, WMCs, mainly in the left hemisphere. Electroencephalography showed bilateral generalized slowing. Sensory evoked potentials were normal. She deteriorated gradually and spent her last years in a nursing home. She died three years after the onset of symptoms. Postmortem brain autopsy revealed a general and slight gyral atrophy accentuated in the frontal lobes (Figure 2A), while the posterior regions showed no surface atrophy. The white matter showed severe frontal and central demyelination, while the parietal-occipital and temporal regions were markedly more spared. Myelin and silver stains revealed massive axonal breakdown as well as near-total demyelination and near-complete loss of axonal structure. Axonal thickenings, occasionally resembling spheroids, were seen, but they were relatively scarce. Spheroid macrophages were scattered, filled with axonal/myelin sheath debris and mildly pigmented. The autopsy revealed swollen, globoid astrocytes in some regions adjacent to better-preserved white matter (Figure 2). We endeavored to extract DNA from paraffin blocks archived at autopsy. However, repeated attempts were unsuccessful due to DNA degradation since the tissue preservation in 2001.

Patient 3. At 42 years of age, the daughter of Patient 2 was admitted to a regional hospital with right arm and leg weakness that had progressed over the course of a month. She had no prior significant medical history. There were no signs of a neuropsychiatric or cognitive dysfunction. At our 18-month follow-up, she was confined to a wheelchair and needed help with most daily activities. She was oriented to time and space. She had severe dysarthria and dysphasia. She exhibited a pseudobulbar syndrome and a marked combined pyramidal–extrapyramidal syndrome. Brain CT showed calcifications in a stepping-stone pattern (Figure 1C). CT-angiography was normal. MRI showed symmetric bilateral atrophy and widespread confluent WMCs (Figure 1C). U-fibers were mostly spared, and the MRI revealed no contrast enhancement. The lesions were essentially unchanged four months later. A spinal cord MRI was normal. Testing for *NOTCH3* gene mutations was negative. The Blueprint Genetics© *CSF1R* single gene test (Version 1, Mar 01, 2018) Plus Analysis identified a heterozygous missense variant c.2329>T, p.Arg777Trp.

Patient 4. A 48-year-old man was referred to a private neurological out-patient department due to dysarthria. Following symptom progression, the patient was referred to a university clinic a year later. Neurological examination revealed dysarthria, dysphagia and numbness of the right arm and left leg as well as subjective breathing difficulty. At a 1-year follow-up, the patient had developed spastic paraparesis, urine incontinence and reduced balance. Due to dysarthria that progressed to anarthria, he used a speech-generating tablet. At our 2-year follow-up, a severe bulbar syndrome with hypersalivation and a slight pseudobulbar component had developed, as well as discrete pyramidal, extrapyramidal and deep sensory symptoms. Brain MRI at the 2-year follow-up revealed confluent WMCs with relatively symmetrical frontoparietal distribution and sparing of the U-fibers (Figures 1C and D). The WMCs affected corticospinal tracts down to the decussation in the pons. The corpus callosum was affected in its isthmus and centrally in the splenium region. The patient had developed moderate frontotemporal atrophy as well as slight to moderate central atrophy. Brain CT did not show any calcifications. The Blueprint Genetics© *CSF1R* single gene test (Version 1, Mar 01, 2018) Plus Analysis identified a heterozygous missense variant c.2329C>T, in the *CSF1R* gene (p.Arg777Trp).

Quantitative outcomes in present case series.

Autophosphorylation assay of the mutations CSF1R p.Arg777Trp and p.Arg782Cys Whereas autophosphorylation Tyr546, Tyr708 and Tyr723 was detectable in cells expressing wild-type CSF1R, little autophosphorylation was observed in cells expressing CSF1R mutations of p.Arg777TRP, p.Arg782Cys and p.Ile794Thr (positive control) (Figure 3).

CSF biomarkers. CSF tau was significantly elevated in Case 1, while CSF beta-amyloid and CSF phosphorylated tau were normal in all cases (Table 2). The tau/phospho-tau ratio in Patient 1 was roughly 28 ng/L, which suggests relatively fast progression. Glial fibrillary protein (GFAP) in Patient 1 was markedly elevated, suggestive of astrocytic damage or activation. CSF-NFL levels were significantly elevated, indicating ongoing severe axonal damage, especially in Patient 1.

Table 2. Cerebrospinal fluid analysis.

Patient CSF analysis	Patient 1	Patient 2	Patient 3	Patient 4		Reference value
Number of months from first symptoms to LP	6	4	2	14	27	-
CSF-tau	1180 ng/L	N/A	240	N/A	N/A	<300 ng/L
CSF-beta-amyloid	934 ng/L	N/A	651	N/A	N/A	>550 ng/L
CSF-phospho-tau	42 ng/L	N/A	19	N/A	N/A	<60 ng/L
CSF-GFAP	5150 ng/L	N/A	400	N/A	N/A	<750 ng/L
CSF-NFL	24300 ng/L	N/A	8840 ng/L	4090 ng/L	5110 ng/L	<890 ng/L**)
CSF-CXCL13	N/A	N/A	N/A	<1.0 ng/L	<1.0 ng/L	<7.8 ng/L
CSF leukocyte count	0	Normal	0	0	0	0–5 x 10(6)/L
CSF albumin ratio	3.3	*)	1.7	6.4	5.7	<9.0 x (10-3)
CSF IgG index	0.45	N/A	0.63	0.45	0.46	<0.7
OCB	absent	N/A	absent	absent	absent	absent

Abbreviations : Ig = immunoglobulin; IL= interleukin; FLC-K = Free light chains type kappa; KFLC = Kappa free light chains; NFL = Neurofilament light; GFAP = glial fibrillary acidic protein; OCB = oligoclonal bands; CXCL = Chemokine (C-X-C motif) ligand; mg = milligram; L = liter; ng = nanogram; N/A = Not available.

Symbols: *) Total protein normal **) age-dependent cut-off;

Function estimation scores (FES). Table 3 presents results of assessment scales that were used to rate patients described in this case series. Figure 4 shows a composite graphic representation of ALSP-FES: a radar chart. It visualizes a reverse relationship between the CSF-NFL level and a set of neurological ALSP-FES. A higher CSF-NFL level corresponds to a lower ALSP-FES score.

Table 3. Function estimation scores (FES)

Estimation Patient instrument, time	Patient 1	Patient 2	Patient 3	Patient 4
Rating time point, years after onset	2 years	N/A	1 year	3 years
UPDRS part I	9	N/A	4	4
UPDRS part II	33	N/A	24	15
UPDRS part III	35	N/A	32	8
UPDRS part IV	N/A	N/A	N/A	N/A
UPDRS part V	Stage 5	N/A	Stage 5	Stage 1
UPDRS part VI	10%	N/A	25%	100%
ALSFRS-R	24	N/A	17	31
HADS Depression/Anxiety	N/A	N/A	9/9	13/9
EQ5D / VAS	10/N/A	N/A	14/10	10/4
EDSS	8.0	N/A	7.5–8.0	5.5
MMSE	N/A	N/A	15	24
MSIS-29	N/A	N/A	N/A	N/A
SDMT	N/A	N/A	N/A	31

Abbreviations: UPDRS = Unified Parkinson's Disease Rating Scale; ALSFRS = ALS Functional Rating Scale; HADS = Hospital Anxiety Depression Rating Scale; EQ5D = EuroQol-5D standardized instrument for measuring generic health status; VAS = Visual Assessment Scale; EDSS = Expanded Disability Status Scale; MMSE = Mini-Mental State Examination; MSIS-29 = Multiple Sclerosis Impact Scale; SDMT = Symbol Digits Modalities Test; N/A = Not Available.

Discussion

In this case series we describe four cases of *CSF1R*-related leukoencephalopathy caused by *CSF1R* gene mutations found in members of three families in Sweden. Patients 3 and 4, who were not related, had a previously known mutation: CSF1R p.Arg777Trp. On the other hand, no researchers have previously reported clinico-pathological or pathogenicity data on the CSF1R p.Arg782Cys mutation in case 1, although the review by Konno et al. (7) briefly mentioned this mutation. In this paper, we report that these *CSF1R* mutants had lost ligand-induced autophosphorylation of CSF1R, which confirms the pathogenicity of

this heterozygous missense mutation. The postmortem tissue biobank at Lund University gave us an outstanding possibility to connect a clinical case with definitive *CSF1R*-related leukoencephalopathy to autopsy findings. Despite brain tissue specimen age, we were able to create workable histopathological images with findings typical for *CSF1R*-related leukoencephalopathy: axonal spheroids and pigmented macrophages (20, 21).

Table 4. Overview of reported cases with mutations CSF1R p.Arg782Xaa and CSF1R p.Arg777Xaa.

Mutation, (reference), nucleotide change	Location	Country	Inheritance	Initial symptoms	Neuroradiology
p.Arg782Cys[a] c.2344C>T	Exon 18	Sweden	Sporadic	Cognitive decline, dysarthria, dysphasia.	Confluent white matter changes with a subtle left-sided predominance, sparing of U-fibers; frontal calcifications.
p.Arg782His (45) c.2345G>A	Exon 18	Japan	Familial	Cognitive decline, aphasia and seizures.	Fronto-temporal atrophy and confluent periventricular white matter changes.
p.Arg782His (46) c.2345G > A	Exon 18	USA	Familial	Cognitive decline, depression and apraxia.	Increased signal on FLAIR and T2-weighted images in the periventricular and deep white matter.
p.Arg782Gly (22) c.2344C > G	Exon 18	UK	Familial	Behavioral changes and paraparesis.	Multifocal involvement of the corpus callosum with volume loss, particularly posteriorly. Asymmetric white matter involvement with sparing of U-fibers. Mild parietal and frontal atrophy.
p.Arg777Trp[a] c.2329C>T	Exon 18	Sweden	Familial/sporadic	Combined pyramidal-extrapyramidal syndrome, pseudobulbar syndrome.	Symmetrical confluent white matter abnormalities with sparing of the U-fibers. The corpus callosum was affected in its isthmus and centrally in the splenium region. Foci of restricted diffusion were present in the periphery of the white matter changes. Moderate frontotemporal atrophy.
p.Arg777Trp (23)	Exon 18	Japan	Familial	Alcoholism, personality	Atrophy in frontal, parietal and medial

N/A				changes and dementia.	temporal lobes, with periventricular confluent hyperintensities.
p.Arg777Gln (20) N/A	Exon 18	France	Familial	Progressive frontal dementia, dysarthria and apraxia.	Frontal and callosal atrophy predominantly with diffuse white matter hyperintensity bilaterally with relative sparing of U fibers.

Abbreviations: [a] = Cases presented in the current study.

Arg = Arginine; Cys = Cysteine; Gln = Glutamine; Gly = Glycine; FLAIR = Fluid-Attenuated Inversion Recovery; His = Histidine; N/A= Not Available; Trp = Tryptophan; UK = United Kingdom.

Table 4 summarizes previously reported cases and families with mutations at CSF1R p.Arg782Xaa and CSF1R p.Arg777Xaa. Different missense changes affecting the 782 amino acid residue indicate that this location is a hot spot, arginine being exchanged with glycine, cysteine, leucine or histidine (5, 7). A change to cysteine at position 782 (Patient 1) may have a stronger physiochemical impact (Grantham score: 180 [0–215] indicating a greater evolutionary distance) than the change to histidine (Grantham score 29 [0–215]) while a change to glycine may have an intermediate impact (Grantham score: 125 [0–215]). Thus, the mutation in our case 1 — p.Arg782Cys, c.2344C>T of the *CSF1R* gene—may predict a more severe disease. Nevertheless, a rapid course was observed in a case with a change to glycine, CSF1R p.Arg782Gly, c2344C>G with a disease duration of only two years and two months (22). The cases with the CSF1R p.Arg777Trp mutations—one likely familiar and the other arguably sporadic—has no family relationship, although we did not explore the patients' ancestral lines. An CSF1R p.Arg777Trp point substitution was previously described as a novel mutation in a Japanese patient with alcoholism, personality changes and dementia (23). The mutation was considered to be likely pathogenic from cross-species conservation. Our autophosphorylation test confirmed the pathogenicity of this specific mutation. Another missense alteration at this residue, CSF1R p.Arg777Gln was described in three individuals from a French family who exhibited progressive frontal dementia, dysarthria and apraxia (20) and in a family with early onset and rapid disease progression of HDLS (24).

We explored the clinical heterogeneity of *CSF1R*-related encephalopathy, integrating scoring systems for extrapyramidal, motor neuron and neuropsychiatric/cognitive functions into a radar chart. Patients with *CSF1R*-related leukoencephalopathy present with a wide range of adult-onset focal or systemic neurological and cognitive symptoms. Previous reports present a spectrum of phenotypes (21), protracted asymptomatic

courses (25), a phenotype with features of progressive MS (26), and patients with parkinsonian features (27), as well as dominant bulbar symptoms as in our case 4 (28). We scored our present cases with a composite of several established FESs used to diagnose specific neurological diseases, which we termed ALSP-FES. We propose this novel radar chart integrated representation of the ALSP-FES as a candidate for assessment of *CSF1R*-related encephalopathy and similar leukodystrophies.

CSF-NFL correlates well with disease activity and disability progression in multiple sclerosis (MS) and is a diagnostic and prognostic biomarker in MS (29, 30). In ALS, CSF-NFL levels correlate with disease progression (31). Hayer et al. reported NFL levels to be considerably elevated in the serum and CSF in *CSF1R*-related leukoencephalopathy (32), with a lack of overlap between patients, and therefore proposed NFL as a valid biomarker. This is consistent with the NFL level in case 1. However, Patients 3 and 4 indicate that CSF-NFL may be only moderately elevated, as commonly seen in MS (relapsing and progressive) and atypical parkinsonism (33-35).

A comparison of Patients 3 and 4 provides an example of possible gender-specific microglia dysfunction (36) that might influence differential temporal involvement of clinical symptoms and severity: Patient 3 was female and presented her first symptoms at age 42, with disease duration of just two months at the CSF sampling time-point. She had higher CSF-NFL concentration and a markedly smaller radar chart area (blue figure) on ALSP-FES (Figure 3B) than Patient 4 (Figure 3C), a male with onset at age 48 and CSF sampling at 14 months of disease duration, who had higher scoring on multiple scales in ALSP-FES (i.e., a better global function). This is consistent with previous observations that female patients tend to develop symptoms earlier (5, 6, 37).

According to Patient 1's neuropsychological assessment, a low premorbid verbal capacity was likely present long before formal diagnosis. His CT scan revealed small frontal calcifications in the frontal region. Hayer et al. found that serum NFL levels were elevated in young, clinically asymptomatic carriers of *CSF1R* mutations (32). Earlier reports indicate that stepping-stone calcifications may exist in advance of HDLS and diminish with age (7). A CT scan performed on a premature patient at one month of age showed frontal calcifications (38). At 24 years of age, when the patient had onset of HDLS, these calcifications had diminished but persisted and had a stepping-stone appearance. However, no genetic traits or clinical features have so far been associated with the stepping-stone calcifications**.**

Recently, Gelfand et al. published a case report in which they describe delayed clinical stabilization of two symptomatic patients with genetically verified *CSF1R*- related leukoencephalopathy after allogenic hematopoietic stem cell transplantation [HSCT, (39), (5)]. Furthermore, some researchers have reported that CSF2 expression is increased in patients with mutant *CSF1R*, making it an attractive therapeutic target (40). In a recent report, the authors proposed that a protracted, nearly asymptomatic course in a patient with a documented *CSF1R* pathogenic mutation was explained by her constant medication with corticosteroids for another disease and the inhibitory effect of the corticosteroids on CSF2's pro-inflammatory effects (41). The recent advancement in genetic engineering techniques, such as CRIPSR gene editing, as well as therapies focused on microglial modulation (42), could potentially offer new treatment avenues in patients with genetic leukoencephalopathies or pre-symptomatic carriers. Because the disease is autosomal dominant

with a high degree of penetrance (5), offspring's risk of being affected is close to 50%. Hypothetically, it could be meaningful to identify such asymptomatic carriers and consider allogenic HSCT at an earlier stage before a full-blown leukoencephalopathy ensues (20), (21).

A weakness of our study is that CSF biomarkers were analyzed in different laboratories that use slightly different methods, which could result in minor discrepancies in values between patients. MRI protocols were not harmonized between different centers.

Conclusions

A precondition for implementing therapy that is still experimental is long-term clinical monitoring with standardized, validated tools to evaluate clinical outcomes and endpoints in these disorders. In this paper, we highlight the variability of *CSF1R*-related leukoencephalopathy semi-quantitatively along the axes of frontal, motor neuron and extrapyramidal disease. We suspect that adult onset leukodystrophies in general, and *CSF1R*-related leukoencephalopathies in particular, are considerably underdiagnosed (43). We intend to increase the awareness of *CSF1R*-related encephalopathies and similar leukodystrophies including AARS- and AARS2-dependent diseases (44) among neurologists and psychiatrists.

Abbreviations

AARS: Alanyl—tRNA synthetase

AARS2: Alanyl—tRNA synthetase 2

ALSFRS: ALS Functional rating scale

ALSP: Adult Leukoencephalopathy with spheroids and pigmented glia

Arg: Arginine

CRISPR: Clustered regularly interspaced short palindromic repeats

CSF: Cerebrospinal fluid

CSF1R: Colony stimulating factor 1 receptor

CT: computed tomography

CXCL: Chemokine (C-X-C motif) ligand

Cys: Cysteine

EDSS: Expanded Disability Status Scale

EQ5D: EuroQol-5D standardized instrument for measuring generic health status

FLAIR: Fluid-attenuated inversion recovery

GCA: Global cortical atrophy

Gd+: Gadolinium enhancing

GFA-p: Glial fibrillary acidic protein

HE: Hematoxylin-eosin

HSCT: Hematopoietic stem cell transplantation

HADS: Hospital Anxiety Depression Rating scale

HDLS: Hereditary diffuse leukoencephalopathy with steroids

Ig: Immunoglobulin

IL: Interleukin

KFLC: Kappa free light chains

L: Liter

LFB: Luxol Fast Blue

Mg: Milligram

MMSE: Mini-Mental Status Examination

MOCA: Montreal cognitive assessment

MOG: Myelin oligodendrocyte glycoprotein

MOG-AD: MOG antibody disease

MRI: Magnetic resonance imaging

MS: Multiple Sclerosis

MSIS-29: Multiple sclerosis impact scale

NA: Not available

NFL: Neurofilament light

Ng: Nanogram

NOTCH3: Neurogenic locus notch homolog protein 3

OCB: Oligoclonal bands

POLD: Pigmentary orthochromatic leukodystrophy

SDMT: Symbol digits modalities test

Trp: Tryptophan

UPDRS: United Parkinson rating scale

VAS: Visual Assessment Scale

WMC: White matter changes

Declarations

Ethics approval and consent to participate. The study was approved by the Regional Ethical Committee in Stockholm, ethical permit Dnr 2009/2017-31/2 “STOPMS-II” (Patient 4) and the Swedish Research Ethics Authority, Ethical permit Dnr 651-05, “HDLS” (Patients 1, 3, 4). Patients signed informed consent to participate in these studies.

Consent for publication. Patients signed consent to publish MRI images and clinical data in this publication.

Availability of data and materials. All data generated or analyzed during this study are included in this published article.

Competing interests. VDK has received financial support from Stockholm County Council (grant ALF 20160457); Biogen (recipient of grant and scholarship, PI for project sponsored by); Novartis (Scientific Advisory board member, recipient of scholarship and lecture honoraria); Merc (Scientific Advisory Board member, recipient of lecture honoraria).

Funding. TI was funded by AMED JP21dk0207045

Authors’ contributions. Study design and conception: OA, IR, VDK. Interpretation of results, design of the work, manuscript drafting and revision: TG, EE, AY, IT, OA, IR , VDK, KJ.

Collection of specific data and interpretation: Histopathology images: EE; MRI images: TG; *In vitro* phosphorylations assay: AY, IT; Radar chart: VDK; Attempted DNA extraction: CH-O; Patients were examined by neurologists: OA, IR, VDK, KJ.

All authors read and approved the final manuscript.

Acknowledgments. We acknowledge the patients and their relatives for participation in the study and consent for this publication. We thank nurses and administrative personnel for help in organizing follow-up visits at university hospitals for our patients. We appreciate Antanas Romas at Vattenfall AB, KSU, Sweden for friendly help with radar charts and mathematical discussion. We appreciate help from biomedical technicians at the Department of Genetics and Pathology, Laboratory Medicine Skåne, Lund, for making brain sections and stainings.

Authors' information. N/A

References

1. Chitu V, Gokhan Ş, Nandi S, Mehler MF, Stanley ER. Emerging Roles for CSF-1 Receptor and its Ligands in the Nervous System. Trends in neurosciences. 2016;39(6):378–93.
2. Guo L, Bertola DR, Takanohashi A, Saito A, Segawa Y, Yokota T, et al. Bi-allelic CSF1R Mutations Cause Skeletal Dysplasia of Dysosteosclerosis-Pyle Disease Spectrum and Degenerative Encephalopathy with Brain Malformation. Am J Hum Genet. 2019;104(5):925–35.
3. Rademakers R, Baker M, Nicholson AM, Rutherford NJ, Finch N, Soto-Ortolaza A, et al. Mutations in the colony stimulating factor 1 receptor (CSF1R) gene cause hereditary diffuse leukoencephalopathy with spheroids. Nat Genet. 2011;44(2):200–5.
4. Nicholson AM, Baker MC, Finch NA, Rutherford NJ, Wider C, Graff-Radford NR, et al. CSF1R mutations link POLD and HDLS as a single disease entity. Neurology. 2013;80(11):1033–40.
5. Konno T, Yoshida K, Mizuno T, Kawarai T, Tada M, Nozaki H, et al. Clinical and genetic characterization of adult-onset leukoencephalopathy with axonal spheroids and pigmented glia associated with CSF1R mutation. Eur J Neurol. 2017;24(1):37–45.
6. Sundal C, Van Gerpen JA, Nicholson AM, Wider C, Shuster EA, Aasly J, et al. MRI characteristics and scoring in HDLS due to CSF1R gene mutations. Neurology. 2012;79(6):566–74.
7. Konno T, Kasanuki K, Ikeuchi T, Dickson DW, Wszolek ZK. CSF1R-related leukoencephalopathy: A major player in primary microgliopathies. Neurology. 2018;91(24):1092–104.
8. Konno T, Yoshida K, Mizuta I, Mizuno T, Kawarai T, Tada M, et al. Diagnostic criteria for adult-onset leukoencephalopathy with axonal spheroids and pigmented glia due to CSF1R mutation. Eur J Neurol. 2018;25(1):142–7.
9. Goetz CG, Fahn S, Martinez-Martin P, Poewe W, Sampaio C, Stebbins GT, et al. Movement Disorder Society-sponsored revision of the Unified Parkinson's Disease Rating Scale (MDS-UPDRS): Process, format, and clinimetric testing plan. Movement disorders: official journal of the Movement Disorder Society. 2007;22(1):41–7.
10. Cedarbaum JM, Stambler N, Malta E, Fuller C, Hilt D, Thurmond B, et al. The ALSFRS-R: a revised ALS functional rating scale that incorporates assessments of respiratory function. BDNF ALS Study Group (Phase III). Journal of the neurological sciences. 1999;169(1–2):13–21.
11. Spinhoven P, Ormel J, Sloekers PP, Kempen GI, Speckens AE, Van Hemert AM. A validation study of the Hospital Anxiety and Depression Scale (HADS) in different groups of Dutch subjects. Psychological

medicine. 1997;27(2):363–70.
12. Kurtzke JF. Rating neurologic impairment in multiple sclerosis: an expanded disability status scale (EDSS). Neurology. 1983;33(11):1444–52.
13. Tombaugh TN, McIntyre NJ. The mini-mental state examination: a comprehensive review. J Am Geriatr Soc. 1992;40(9):922–35.
14. Shi D, Chen X, Li Z. Diagnostic test accuracy of the Montreal Cognitive Assessment in the detection of post-stroke cognitive impairment under different stages and cutoffs: a systematic review and meta-analysis. Neurological sciences: official journal of the Italian Neurological Society of the Italian Society of Clinical Neurophysiology. 2018;39(4):705–16.
15. Strober L, DeLuca J, Benedict RH, Jacobs A, Cohen JA, Chiaravalloti N, et al. Symbol Digit Modalities Test: A valid clinical trial endpoint for measuring cognition in multiple sclerosis. Multiple sclerosis (Houndmills, Basingstoke, England). 2019;25(13):1781–90.
16. Hobart J, Lamping D, Fitzpatrick R, Riazi A, Thompson A. The Multiple Sclerosis Impact Scale (MSIS-29): a new patient-based outcome measure. Brain. 2001;124(Pt 5):962–73.
17. Balestroni G, Bertolotti G. [EuroQol-5D (EQ-5D): an instrument for measuring quality of life]. Monaldi archives for chest disease = Archivio Monaldi per le malattie del torace. 2012;78(3):155–9.
18. Miura T, Mezaki N, Konno T, Iwasaki A, Hara N, Miura M, et al. Identification and functional characterization of novel mutations including frameshift mutation in exon 4 of CSF1R in patients with adult-onset leukoencephalopathy with axonal spheroids and pigmented glia. J Neurol. 2018;265(10):2415–24.
19. Pasquier F, Leys D, Weerts JG, Mounier-Vehier F, Barkhof F, Scheltens P. Inter- and intraobserver reproducibility of cerebral atrophy assessment on MRI scans with hemispheric infarcts. European neurology. 1996;36(5):268–72.
20. Guerreiro R, Kara E, Le Ber I, Bras J, Rohrer JD, Taipa R, et al. Genetic analysis of inherited leukodystrophies: genotype-phenotype correlations in the CSF1R gene. JAMA neurology. 2013;70(7):875–82.
21. Lynch DS, Jaunmuktane Z, Sheerin UM, Phadke R, Brandner S, Milonas I, et al. Hereditary leukoencephalopathy with axonal spheroids: a spectrum of phenotypes from CNS vasculitis to parkinsonism in an adult onset leukodystrophy series. J Neurol Neurosurg Psychiatry. 2016;87(5):512–9.
22. Foulds N, Pengelly RJ, Hammans SR, Nicoll JA, Ellison DW, Ditchfield A, et al. Adult-Onset Leukoencephalopathy with Axonal Spheroids and Pigmented Glia Caused by a Novel R782G Mutation in CSF1R. Scientific reports. 2015;5:10042.
23. Mitsui J, Matsukawa T, Ishiura H, Higasa K, Yoshimura J, Saito TL, et al. CSF1R mutations identified in three families with autosomal dominantly inherited leukoencephalopathy. American journal of medical genetics Part B Neuropsychiatric genetics: the official publication of the International Society of Psychiatric Genetics. 2012;159b(8):951–7.
24. Hoffmann S, Murrell J, Harms L, Miller K, Meisel A, Brosch T, et al. Enlarging the nosological spectrum of hereditary diffuse leukoencephalopathy with axonal spheroids (HDLS). Brain Pathol. 2014;24(5):452–8.

25. La Piana R, Webber A, Guiot MC, Del Pilar Cortes M, Brais B. A novel mutation in the CSF1R gene causes a variable leukoencephalopathy with spheroids. Neurogenetics. 2014;15(4):289–94.
26. Granberg T, Hashim F, Andersen O, Sundal C, Karrenbauer VD. Hereditary diffuse leukoencephalopathy with spheroids - a volumetric and radiological comparison with multiple sclerosis patients and healthy controls. Eur J Neurol. 2016;23(4):817–22.
27. Sundal C, Fujioka S, Van Gerpen JA, Wider C, Nicholson AM, Baker M, et al. Parkinsonian features in hereditary diffuse leukoencephalopathy with spheroids (HDLS) and CSF1R mutations. Parkinsonism Relat Disord. 2013;19(10):869–77.
28. Inui T, Kawarai T, Fujita K, Kawamura K, Mitsui T, Orlacchio A, et al. A new CSF1R mutation presenting with an extensive white matter lesion mimicking primary progressive multiple sclerosis. Journal of the neurological sciences. 2013;334(1–2):192–5.
29. Comabella M, Sastre-Garriga J, Montalban X. Precision medicine in multiple sclerosis: biomarkers for diagnosis, prognosis, and treatment response. Curr Opin Neurol. 2016;29(3):254–62.
30. Khalil M, Teunissen CE, Otto M, Piehl F, Sormani MP, Gattringer T, et al. Neurofilaments as biomarkers in neurological disorders. Nature reviews Neurology. 2018;14(10):577–89.
31. Poesen K, Van Damme P. Diagnostic and Prognostic Performance of Neurofilaments in ALS. Front Neurol. 2018;9:1167.
32. Hayer SN, Krey I, Barro C, Rössler F, Körtvelyessy P, Lemke JR, et al. NfL is a biomarker for adult-onset leukoencephalopathy with axonal spheroids and pigmented glia. Neurology. 2018;91(16):755–7.
33. Novakova L, Axelsson M, Khademi M, Zetterberg H, Blennow K, Malmeström C, et al. Cerebrospinal fluid biomarkers as a measure of disease activity and treatment efficacy in relapsing-remitting multiple sclerosis. Journal of neurochemistry. 2017;141(2):296–304.
34. Williams T, Zetterberg H, Chataway J. Neurofilaments in progressive multiple sclerosis: a systematic review. J Neurol. 2020.
35. Parnetti L, Gaetani L, Eusebi P, Paciotti S, Hansson O, El-Agnaf O, et al. CSF and blood biomarkers for Parkinson's disease. Lancet Neurol. 2019;18(6):573–86.
36. Kodama L, Gan L. Do Microglial Sex Differences Contribute to Sex Differences in Neurodegenerative Diseases? Trends Mol Med. 2019;25(9):741–9.
37. Tian WT, Zhan FX, Liu Q, Luan XH, Zhang C, Shang L, et al. Clinicopathologic characterization and abnormal autophagy of CSF1R-related leukoencephalopathy. Translational neurodegeneration. 2019;8:32.
38. Konno T, Broderick DF, Mezaki N, Isami A, Kaneda D, Tashiro Y, et al. Diagnostic Value of Brain Calcifications in Adult-Onset Leukoencephalopathy with Axonal Spheroids and Pigmented Glia. AJNR American journal of neuroradiology. 2017;38(1):77–83.
39. Gelfand JM, Greenfield AL, Barkovich M, Mendelsohn BA, Van Haren K, Hess CP, et al. Allogeneic HSCT for adult-onset leukoencephalopathy with spheroids and pigmented glia. Brain. 2020;143(2):503–11.
40. Chitu V, Biundo F, Shlager GGL, Park ES, Wang P, Gulinello ME, et al. Microglial Homeostasis Requires Balanced CSF-1/CSF-2 Receptor Signaling. Cell reports. 2020;30(9):3004–19.e5.

41. Tipton PW, Stanley ER, Chitu V, Wszolek ZK. Is Pre-Symptomatic Immunosuppression Protective in CSF1R-Related Leukoencephalopathy? Movement disorders: official. journal of the Movement Disorder Society. 2021;36(4):852–6.
42. Han J, Sarlus H, Wszolek ZK, Karrenbauer VD, Harris RA. Microglial replacement therapy: a potential therapeutic strategy for incurable CSF1R-related leukoencephalopathy. Acta neuropathologica communications. 2020;8(1):217.
43. Hillert J, Stawiarz L. The Swedish MS registry – clinical support tool and scientific resource. Acta Neurol Scand. 2015;132(199):11–9.
44. Sundal C, Carmona S, Yhr M, Almström O, Ljungberg M, Hardy J, et al. An AARS variant as the likely cause of Swedish type hereditary diffuse leukoencephalopathy with spheroids. Acta neuropathologica communications. 2019;7(1):188.
45. Kinoshita M, Yoshida K, Oyanagi K, Hashimoto T, Ikeda S. Hereditary diffuse leukoencephalopathy with axonal spheroids caused by R782H mutation in CSF1R: case report. Journal of the neurological sciences. 2012;318(1–2):115–8.
46. Robinson JL, Suh E, Wood EM, Lee EB, Coslett HB, Raible K, et al. Common neuropathological features underlie distinct clinical presentations in three siblings with hereditary diffuse leukoencephalopathy with spheroids caused by CSF1R p.Arg782His. Acta neuropathologica communications. 2015;3:42.

Figures

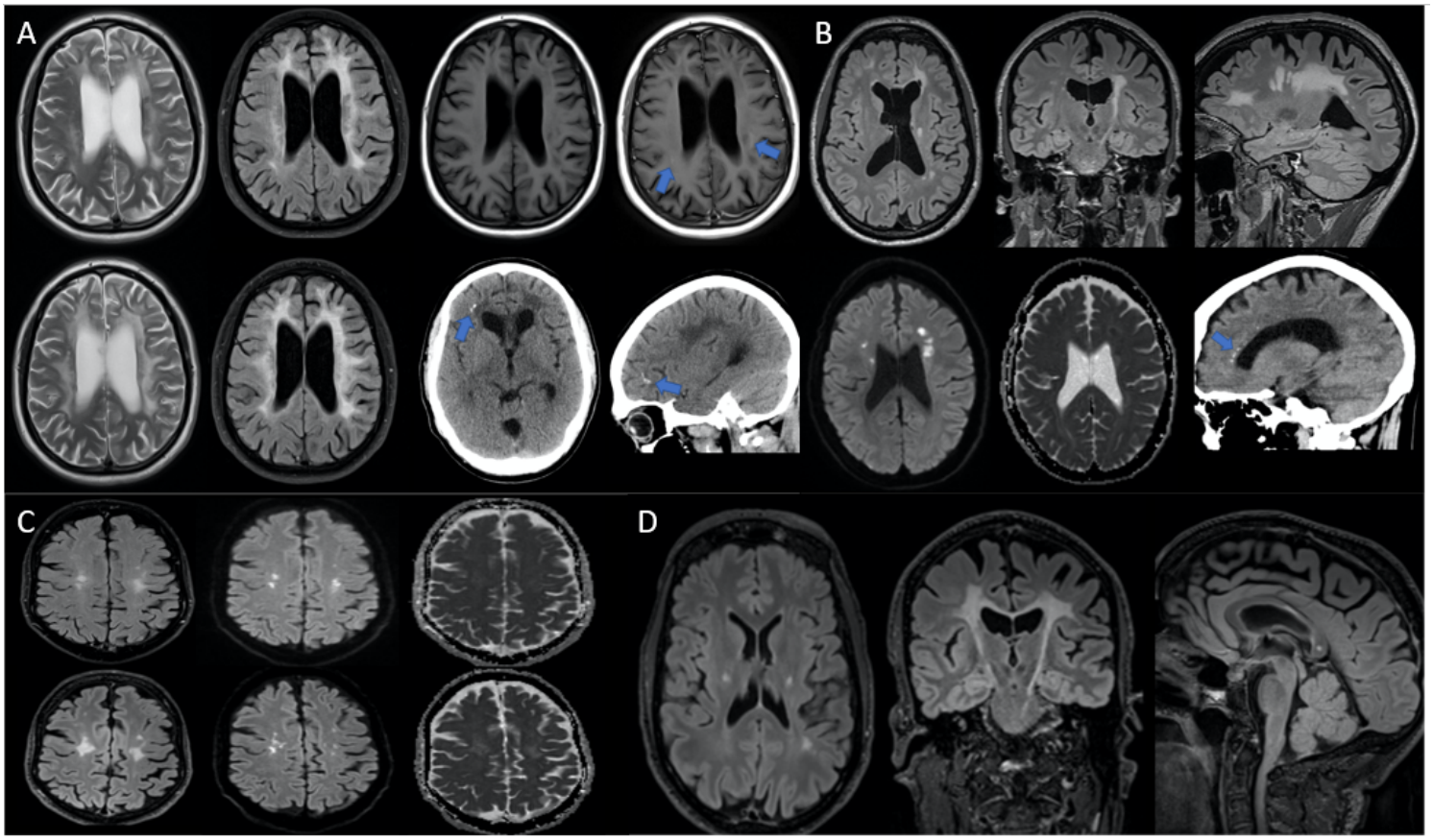

Figure 1

Brain MRI and CT scan images A: Axial T2-weighted (first column) and T2-weighted FLAIR (second column) images showing progression of confluent white matter changes with a subtle left-sided predominance between the baseline scan (top row) at 42 years of age and 10 months later (bottom row). At baseline, T1-weighted imaging (top two right panels) demonstrated very subtle peripheral foci of contrast enhancement at the leading edge (arrows). Small calcifications were seen frontally on the right side on computed tomography (CT, bottom two right panels). Small foci of persistent diffusion restriction were also seen (not shown); B, top row: Axial (left), coronal (middle) and sagittal (right) T2-weighted FLAIR images at 41 years of age showing symmetric confluent white matter hyperintensities sparing the subcortical U-fibers with a prominent involvement of the corticospinal tracts and a left-sided predominance. Bottom row: Diffusion-weighted b1000 (left) and apparent diffusion coefficient (middle) images demonstrated foci of restricted diffusion that persisted four months later at a follow-up (not shown). CT (right) showing multiple punctate calcifications in a “stepping-stone” pattern along the corpus callosum (arrow); C: Axial T2-weighted FLAIR (first column), diffusion-weighted (second column) and apparent diffusion coefficient (third column) images at 48 years of age (top row) and 2.5 years later (bottom row) showing progression of relatively symmetric bifrontal white matter hyperintensities with foci of persistent diffusion restriction at the leading edge. No corresponding calcifications were seen in the brain parenchyma (not shown); D: Axial (left), coronal (middle) and sagittal (right) T2-weighted FLAIR images at 51 years of age showing symmetric confluent white matter hyperintensities sparing the subcortical U-fibers with a prominent involvement of the corticospinal tracts and the central portion of the splenium of corpus callosum.

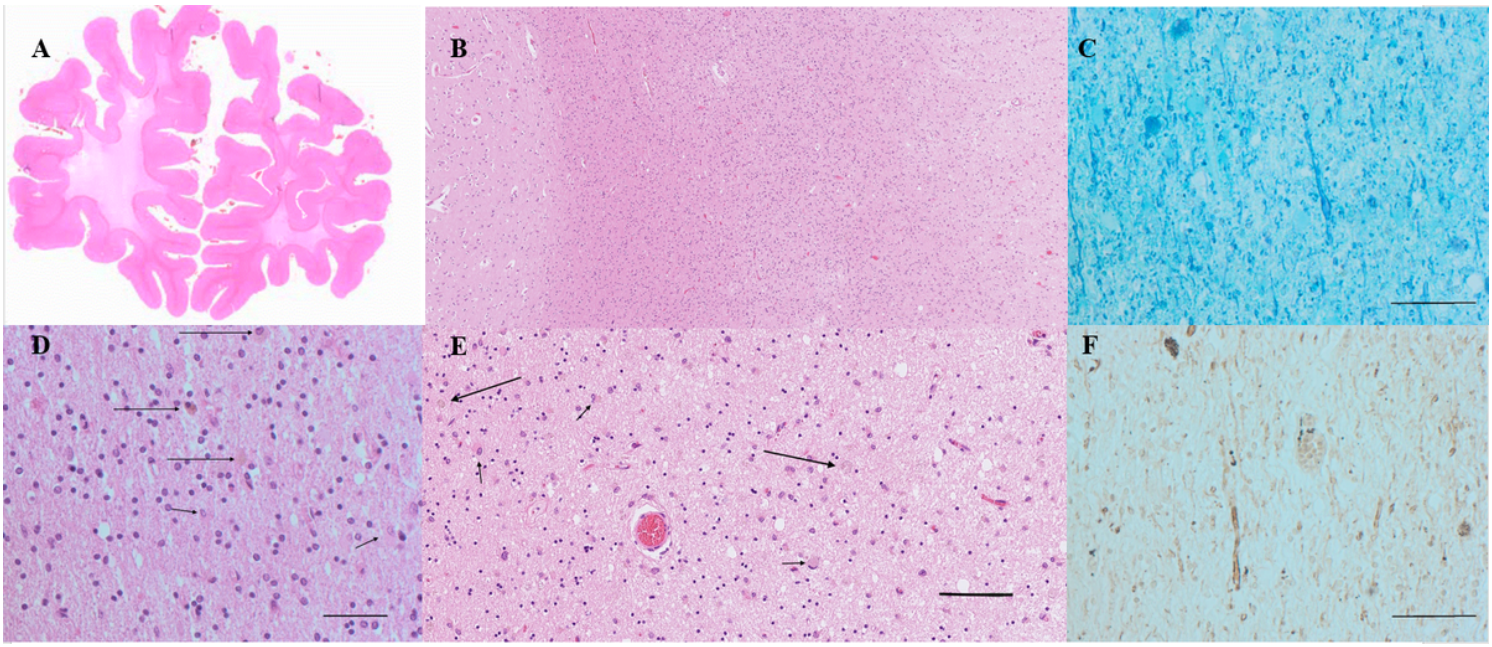

Figure 2

Histopathology of Patient 2 postmortem brain tissue sections. A: Macrophotograph of a coronal section from the anterior frontal lobes of case 2, hematoxylin-eosin staining. Note the well-delineated cortical ribbon, which is of normal width and the subjacent white matter, which is severely attenuated and therefore causing shrinkage of the entire frontal lobe on both sides; B: Microphotograph at low magnification of the border cortex-white matter in the posterior frontal lobe, left hemisphere, hematoxylin-eosin. Note the intact cortical tissue with dense and preserved matrix (left) and the relatively preserved subcortical white matter (center),

while deeper white matter is markedly attenuated (right); C: Microphotograph of the pathological frontal white matter, Luxol Fast Blue - Cresyl violet myelin staining. This area is within the anterior frontal lobe (A). Note the extreme scarcity of myelin sheaths and the axonal and myelin sheath swelling in one of the few remaining long structures; D: A white matter area from the posterior frontal lobes (behind the region of maximal damage, as in B), showing an attenuated white matter with many reactive astrocytes and a few mildly pigmented macrophages. Hematoxylin-eosin; E: An area with more severe damage: pleomorphic reactive cells (astrocytes and macrophages) and a more attenuated matrix. F: Attenuated white matter from the anterior frontal lobe, as in A and C, Gallyas silver staining for identification of axons. Note the rudimental fragments of axons and the two macrophages (pigmented) with granular intracellular debris. Bar indicates 0.05 mm.

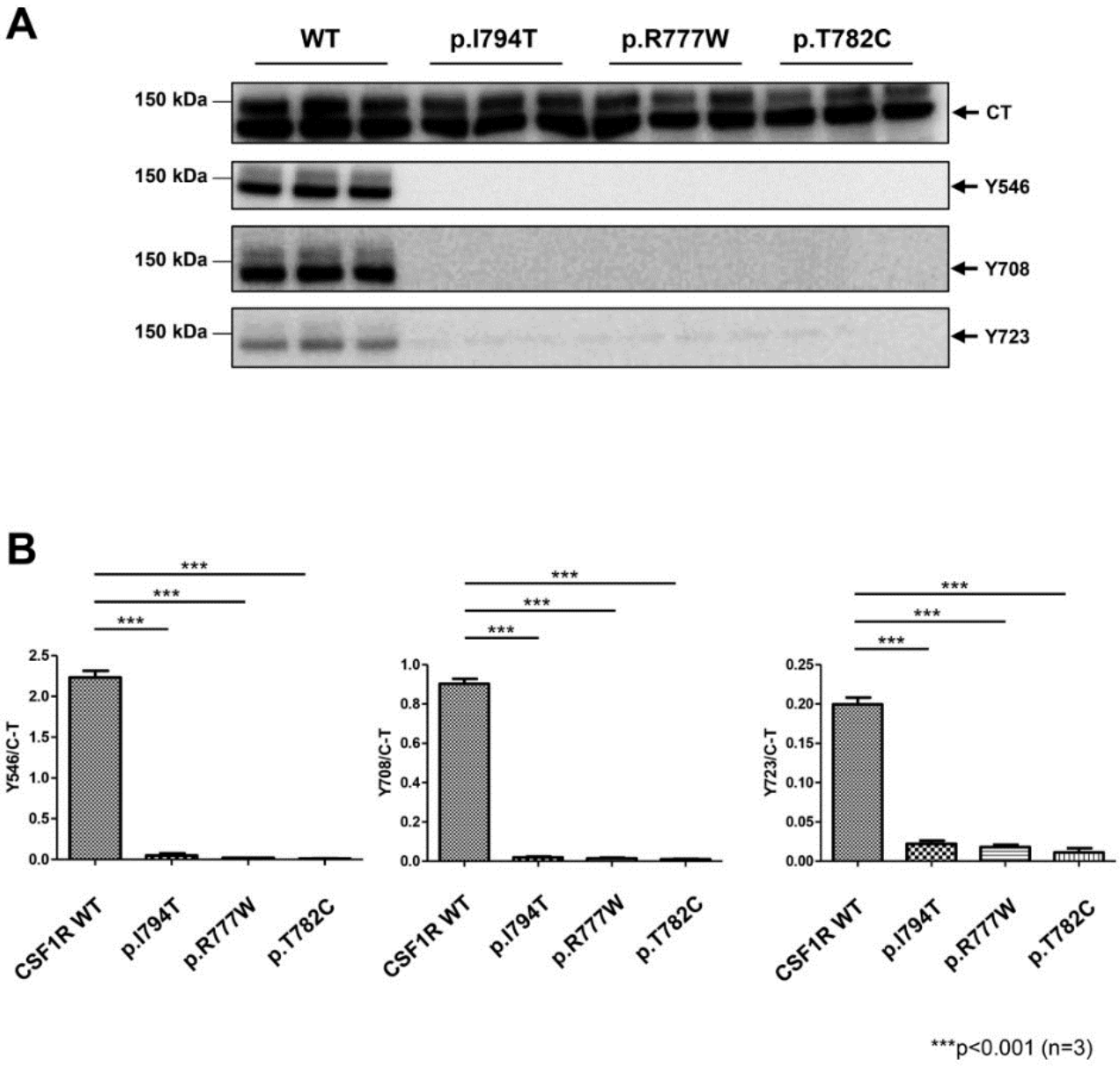

Figure 3

In vitro functional assay of mutant CSF1Rs 3A: Ligand-dependent autophosphorylation of CSF1R was examined in cells transfected with wild-type or variant CSF1Rs. The mutation of CSF1R p.Ile794Thr was

frequently identified in patients with ALSP (5) and is known to be pathogenic as has been previously reported (18). Although phosphorylation of CSF1R at Tyr546, Tyr708 and Tyr723 was observed in cells expressing wild-type CSF1R after ligand (CSF1) stimulation, neither of the CSF1R mutants underwent autophosphorylation. 3B: The signal intensity of immunoblot was semi-quantitatively analyzed. Each autophosphorylation signal of CSF1R was normalized by the signal from the total amount of CSF1R. Horizontal bars indicate the difference between wild-type and the positive control as well as the mutations in the patients presented here. Data are presented as mean±SEM.

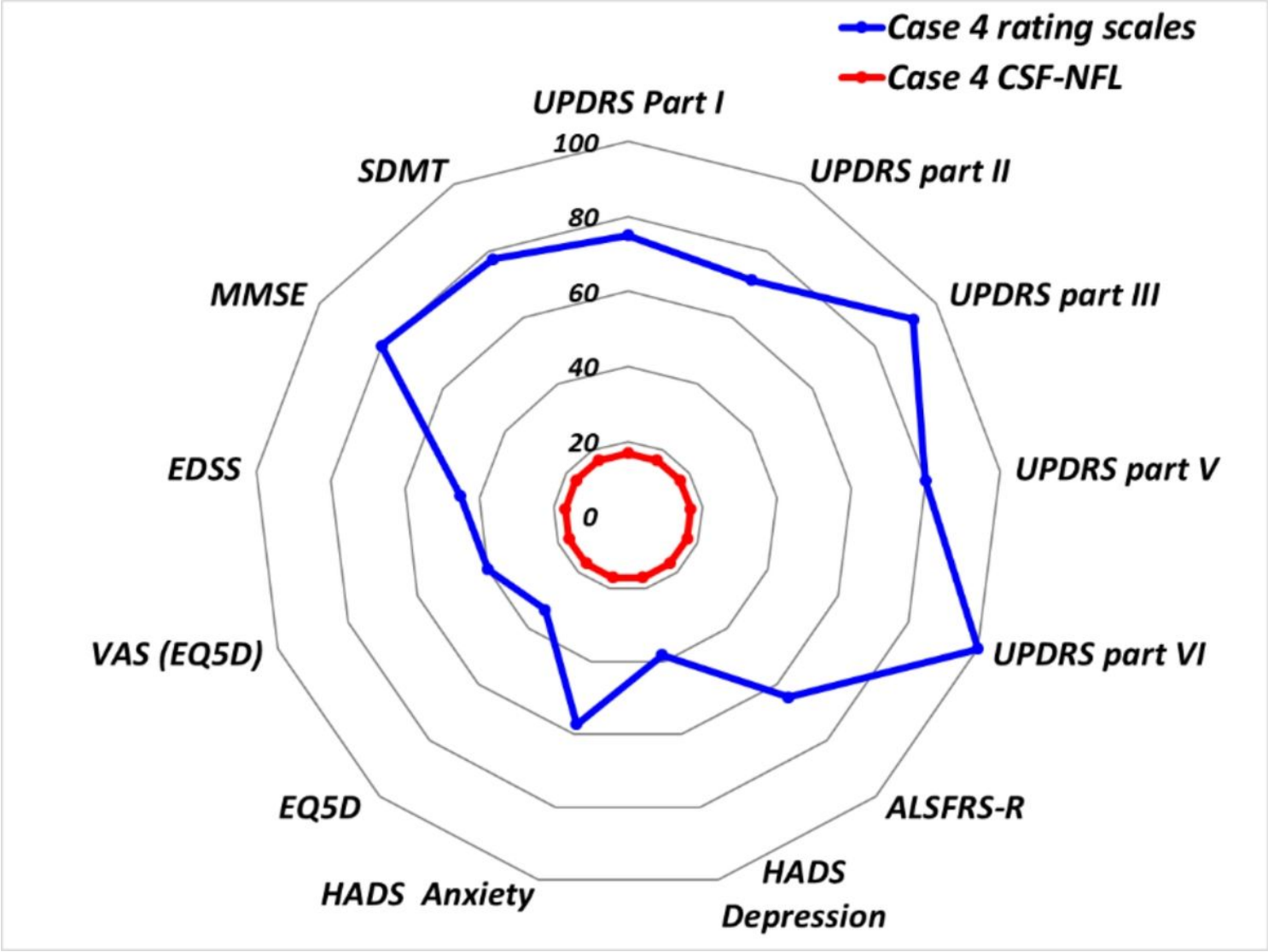

Figure 4

Radar chart visualizing symptoms assessed with FES and CSF-NFL levels Visualization of the relationship between CSF-NFL and the variation in function estimate scores for each case. The center of a blue figure represents the least relative function of a patient, and blue dots localized further from the center represent better function on the specific evaluation scale. Red dots and lines denote the relative value of CSF-NFL at diagnosis., normalized as 100% for case 1 (24.300 ng/L) and presented as relative percentage for cases 3 and 4.

Supplementary Files

This is a list of supplementary files associated with this preprint. Click to download.

- Supplement1.docx
- Supplement2.docx
- Supplement3.xlsx
- Supplement4.docx